Document made available under the Patent Cooperation Treaty (PCT)

International application number: PCT/AU04/001704

International filing date: 03 December 2004 (03.12.2004)

Document type: Certified copy of priority document

Document details: Country/Office: AU
Number: 2003906690
Filing date: 03 December 2003 (03.12.2003)

Date of receipt at the International Bureau: 04 January 2005 (04.01.2005)

Remark: Priority document submitted or transmitted to the International Bureau in compliance with Rule 17.1(a) or (b)

World Intellectual Property Organization (WIPO) - Geneva, Switzerland
Organisation Mondiale de la Propriété Intellectuelle (OMPI) - Genève, Suisse

PCT/AU2004/001704

Australian Government

Patent Office
Canberra

I, JANENE PEISKER, TEAM LEADER EXAMINATION SUPPORT AND SALES hereby certify that annexed is a true copy of the Provisional specification in connection with Application No. 2003906690 for a patent by AUSTRALIAN TELECOMMUNICATIONS COOPERATIVE RESEARCH CENTRE as filed on 03 December 2003.

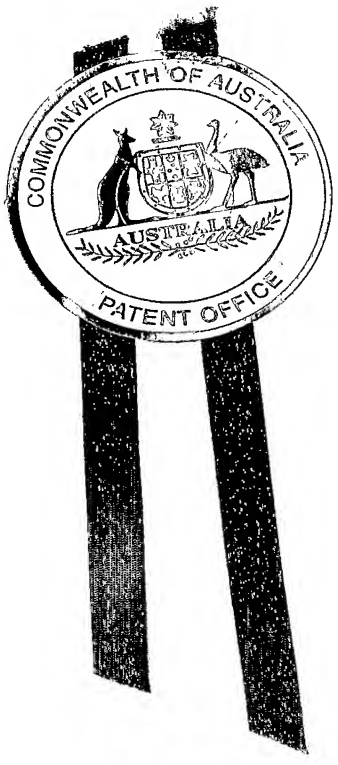

WITNESS my hand this
Twenty-second day of December 2004

JANENE PEISKER
TEAM LEADER EXAMINATION
SUPPORT AND SALES

Provisional Patent Application

Igor Tolochko and Mike Faulkner
Victoria University, ATcrc
PO Box 14428
Melbourne City VIC 8001, Australia

01/12/03

Channel estimation for orthogonal frequency-division multiplexing systems

Abstract

The linear minimum mean-squared error (LMMSE) channel estimator for orthogonal frequency-division multiplexing (OFDM) systems requires large number of complex multiplications. LMMSE channel estimation by significant weight catching (SWC) algorithm can significantly reduce computational complexity of the full LMMSE channel estimator and it outperforms the LMMSE channel estimation by singular value decomposition (SVD) in channels with large delay spreads. The LMMSE channel estimator and its sparse approximations complexity can be further reduced if the channel's exponential power delay profile is approximated as a uniform. The latter approach makes all the coefficients of the fixed weighting matrix real, if the channel impulse response (CIR) is located symmetric around zero by a cyclic shift. Alternatively, real and imaginary parts of the uniform fixed weighting matrix values are made to contain equal or zero entries, when 'good' cyclic prefix (CP) length windows are chosen and cyclic shift is not required.

Outline

1. A method for channel estimation is disclosed in Attachment 1: I. Tolochko and M. Faulkner, "Sparse Approximations in the LMMSE Channel Estimator for OFDM with Transmitter Diversity".
2. The LMMSE channel estimation by significant weight catching (SWC) algorithm can be used in any single-input single-output (SISO) or multiple-input multiple-output (MIMO) OFDM communication system.
3. Any of the three pilot symbol allocation schemes can be applied for channel estimation. Refer Attachment 2: I. Tolochko and M. Faulkner, "Channel Estimation in Wireless LANs with Transmitter Diversity".
4. A switched look-up-table (LUT) approach can further improve the estimation accuracy. Refer to: I. Tolochko and M. Faulkner, "Real Time LMMSE Channel Estimation for Wireless OFDM Systems with Transmitter Diversity", in Proc. 56th IEEE VTC, Vancouver, Canada, pp. 1555 - 1559, 2002.
5. Channel estimator complexity can be further reduced, if the channel's exponential power delay profile is approximated as a uniform, when 'good' cyclic prefix (CP) length windows are chosen.
6. With the uniform power delay profile, coefficients of the fixed weighting matrix can be made real, if the channel impulse response (CIR) is located symmetric around zero by a cyclic shift, as shown in Fig. 1. This reduces the number of multiplications and additions required. The cyclic shift of the CIR can be done in the time domain or in the frequency domain.

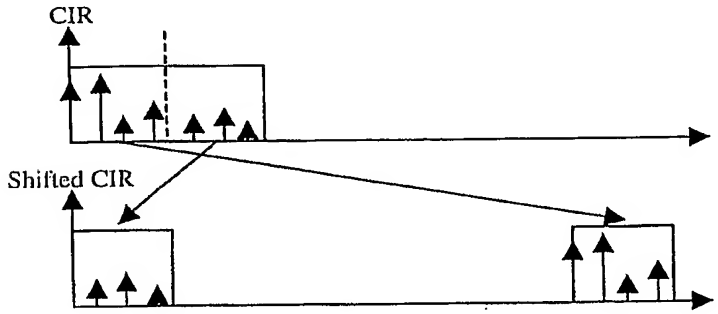

Fig. 1

7. The channel estimation algorithms flowchart is presented in Fig. 2. CIR rotation is performed in the frequency domain.

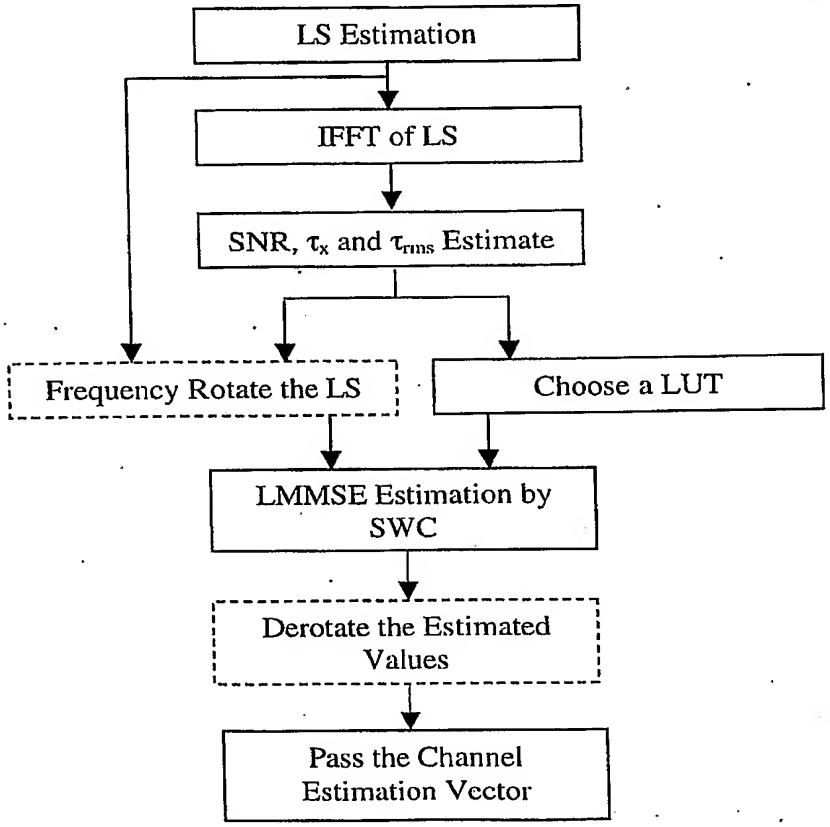

Fig. 2

8. If the 'good' CP windows are used, algorithm steps in the dashed boxes are not required. However, the latter approach can reduce the quality of the estimator due to an imperfect windowing of the CIR.

Sparse Approximations in the LMMSE Channel Estimator for OFDM with Transmitter Diversity

I. Tolochko, *Student Member, IEEE*, and M. Faulkner, *Member, IEEE*

Abstract— The linear minimum mean-squared error (LMMSE) channel estimator for orthogonal frequency-division multiplexing (OFDM) systems requires large number of complex multiplications. In this letter, we evaluate LMMSE channel estimation by significant weight catching (SWC) algorithm for OFDM with transmitter diversity. The new algorithm can reduce computational complexity of the traditional LMMSE channel estimator by more than 50% and it outperforms the LMMSE channel estimation by singular value decomposition (SVD) in HIPERLAN/2 channels with delay spreads exceeding 50 ns.

Index Terms—channel estimation, linear minimum mean-squared error (LMMSE), orthogonal frequency-division multiplexing (OFDM).

1 Introduction

We consider OFDM-based wireless local area networks (WLANs) in a downlink diversity environment with 2 transmitters and 1 receiver. To enable channel estimation, pilot symbols can be simultaneously sent from 2 transmit antennas on interleaved sub-carries. At the receiver end, the LMMSE channel estimator can identify channel characteristics in the non-measured sub-channels by interpolating the different sets of measured sub-channels from the specified antenna [1]. Therefore, in an OFDM system with K used sub-carriers, $K/2$ complex multiplications are required per tone.

Other authors have evaluated sparse approximations of the discrete Fourier transform (DFT) based estimators in [2]. However, the DFT-based estimators have limited performance for non-sample-spaced channels and high signal-to-noise ratios (SNR's) [3]. A low complexity LMMSE channel estimation by SVD has also been investigated in [3]. The estimator complexity can be reduced from $K/2$ to $3r/2$, but the choice of r depends on the fading channel delay spread. Larger delay spreads in a channel require higher rank-r estimator to reduce the mean square error (MSE) floor at high SNRs. In the following section, we evaluate an alternative sparse approximation of the fixed weighting matrix for the LMMSE channel estimation.

2 Sparse Approximations of the Fixed Weighting Matrix

2.1 System Model

The two transmit antennas $j = 1, 2$ simultaneously send two OFDM pilot symbols on K interleaved sub-carriers. The pilot symbols are defined as follows

$$\begin{aligned} \mathbf{x}_1 &= \{a_0,\ 0,\ a_1,\ 0,\ a_2,\ \ldots,\ a_{K/2-1},\ 0\} \\ \mathbf{x}_2 &= \{0,\ b_0,\ 0,\ b_1,\ 0,\ b_2,\ \ldots,\ 0,\ b_{K/2-1}\}. \end{aligned} \tag{1}$$

where a_k and b_k are arbitrary complex numbers with magnitude of 1.

Each of these signals forms an OFDM block. With the channel impulse response confined to a cyclic prefix (CP) length, the DFT of the received symbols can be given by

$$y(k) = \sum_{j=1}^{2} H_j(k)x_j(k) + v(k) \tag{2}$$

where $k = 0,\ 1,\ \ldots,\ K-1$ denotes the sub-carrier number, $H_j(k)$ is the channel frequency response corresponding to transmit antenna j and $v(k)$ is the additive complex Gaussian noise with zero mean and variance one.

We assume packet-type channel estimators, where only the frequency correlation of the channel is used in the estimation. The frequency domain correlation depends on the multipath channel delay spread [2] and can be described by a frequency domain correlation function $r_f(k)$. For an exponentially decaying multipath power delay profile $r_f(k)$ can be given by [4]

$$r_f(k) = \frac{1}{1 + j2\pi\tau_{rms}k(\Delta f)} \tag{3}$$

where τ_{rms} is the root-mean square (rms) delay spread of the power delay profile and Δf denotes the sub-carrier spacing.

2.2 Channel Estimation

In OFDM-based WLANs, a binary phase-shift keying (BPSK) modulation type is generally used to enable channel estimation [5]. Therefore, the LMMSE channel estimation vector $\hat{\mathbf{H}}_j$ corresponding to the jth transmitter in a 2×1 diversity system can be obtained as follows [4]

$$\hat{\mathbf{H}}_j = \mathbf{R}_{\mathbf{H}_j\tilde{\mathbf{P}}_j}\mathbf{R}^{-1}_{\tilde{\mathbf{P}}_j\tilde{\mathbf{P}}_j}\tilde{\mathbf{P}}_j \tag{4}$$

where $\mathbf{R}_{\mathbf{H}_j\tilde{\mathbf{P}}_j} = \mathbf{R}_{\mathbf{H}_j\mathbf{P}_j}$ and $\mathbf{R}_{\tilde{\mathbf{P}}_j\tilde{\mathbf{P}}_j} = (\mathbf{R}_{\mathbf{P}_j\mathbf{P}_j} + \frac{1}{SNR}\mathbf{I})$ are the correlation matrices of size $K \times K/2$ and $K/2 \times K/2$ respectively [3]. $\mathbf{I}$ is the identity matrix and SNR is the expected

value of SNR. $\tilde{\mathbf{P}}_j$ is the least-squares (LS) estimation vector of length $K/2$ at the pilot positions corresponding to antenna j, given by

$$\tilde{\mathbf{P}}_j = \mathbf{X}_j^{-1}\mathbf{y}_j \tag{5}$$

where $\mathbf{X}_j$ is a diagonal matrix containing the transmitted pilot points $x_j(k)$ given by (1).

The best low-rank approximation of $\mathbf{R}_{\mathbf{H}_j\mathbf{P}_j}\mathbf{R}^{-1}_{\tilde{\mathbf{P}}_j\tilde{\mathbf{P}}_j}\mathbf{R}^{1/2}_{\tilde{\mathbf{P}}_j\tilde{\mathbf{P}}_j}$ is given by the SVD [6]. Then, with the appropriate substitutions in (4), the rank-r estimator is defined by

$$\hat{\mathbf{H}}_j = \mathbf{U}_j \begin{bmatrix} \mathbf{\Sigma}_j^r & 0 \\ 0 & 0 \end{bmatrix} \mathbf{V}_j^H \mathbf{R}^{-1/2}_{\tilde{\mathbf{P}}_j\tilde{\mathbf{P}}_j}\tilde{\mathbf{P}}_j \tag{6}$$

where $\mathbf{U}_j$ and $\mathbf{V}_j^H$ are unitary matrices, and $\mathbf{\Sigma}_j^r$ is the $r \times r$ upper left corner diagonal matrix, containing the strongest singular values. The superscripts $(\cdot)^r$ and $(\cdot)^H$ denote rank-r and Hermitian transpose respectively.

In channels with large delay spreads, the rank-r needs to be sufficiently large to eliminate the MSE error floor above a given SNR range. When the rank-r approaches a value of $K/3$, the low rank approximation no longer reduces the estimator complexity.

Based on these observations, an alternative sparse approximation of the fixed weighting matrix, namely LMMSE by significant weight catching (SWC), is evaluated below. For notational convenience, we can rewrite (4) as

$$\hat{\mathbf{H}}_j = \mathbf{W}_j\tilde{\mathbf{P}}_j \tag{7}$$

where $\mathbf{W}_j = \mathbf{R}_{\mathbf{H}_j\tilde{\mathbf{P}}_j}\mathbf{R}^{-1}_{\tilde{\mathbf{P}}_j\tilde{\mathbf{P}}_j}$ is the fixed weighting matrix.

Obviously, some row entries of the $\mathbf{W}_j$ contain stronger weights than the others, with the strongest values on its diagonal. This is illustrated in Fig. 1 for four arbitrary chosen rows. The $\mathbf{W}_j$ was generated using (3) for 64-point OFDM with sampling rate of fs = 20 MHz, at

SNR = 30 dB and $\tau_{rms} = 50$ ns.

Our approach is to restrict the frequency domain $\mathbf{W}_j$ to be a sparse smoothing matrix containing the M strongest weights in each row, where $M \leq K/2$. Hence

$$E_j(k) = \arg\max_{w_j(k,m)} \left\{ \left(\sum_{m=0}^{M-1} |w_j(k,m)|^2 \right) \middle| \mathbf{w}_j(k) \right\} \tag{8}$$

where $\mathbf{w}_j(k)$ denotes a row vector from the smoothing matrix.

3 Numerical Results

Simulations were carried out in an 802.11a system with 2 transmitters and 1 receiver. The MSE for antenna j is given by [3]

$$MSE_j = \frac{1}{K} trace \left(E \left\{ \left(\hat{\mathbf{H}}_j - \mathbf{H}_j \right) \left(\hat{\mathbf{H}}_j - \mathbf{H}_j \right)^H \right\} \right). \tag{9}$$

The system operated in an indoor HIPERLAN/2 non-sample-spaced channels A ($\tau_{rms} =$ 50 ns), B ($\tau_{rms} = 100$ ns) and C ($\tau_{rms} = 150$ ns) [7], with the total transmit power normalized to unity. It was assumed that perfect knowledge of the SNR and τ_{rms} were available for calculation of the $\mathbf{W}_j$.

The MSE channel estimation performance was evaluated by transmitting two long OFDM-BPSK pilot symbols through a fading multipath channel 1000 times. For each iteration, the pilot symbols were simultaneously sent from the two transmit antennas on interleaved sub-carriers. The duration of the two long pilots was 8 μs including double-length CP of 1.6 μs and the total system bandwidth was subdivided into $K = 52$ sub-carriers (out of a possible 64) [5]. For the sparse approximations, the number of complex multipliers ($M < K/2$) was chosen to give targeted MSE error floor ≤ -25 dB.

It was observed that the LMMSE by SVD outperforms the LMMSE by SWC in channel A, when the rank $r \geq 8$, Fig. 2. At a fixed value of SNR = 25 dB, its MSE error floor is well

below of 25 dB and the estimator requires 12 complex multipliers. However, if the channel's delay spread is increased (channels B and C), the LMMSE by SWC is a better compromise in performance versus complexity, as shown in Fig. 2. The LMMSE by SWC requires only 12 complex multipliers in order to reach an adequate performance in channel B and the estimator complexity is reduced by more than 50% compare to the full LMMSE. It is also worth mentioning that the performance of the simplified LMMSE algorithm remains almost unchanged in all the channels, especially for the low number of complex multipliers ($\leq$ 12). To illustrate the performance for a dynamic SNR range, the MSE in channel B is presented in Fig. 3. The number of complex multipliers $M = 3\tau/2$ in the sparse approximations was set to the fixed nominal values of 12 and 21. With the MSE gain of 9 dB over the LMMSE by SVD for $M =$ 12 at SNR = 30 dB, it is obvious that the LMMSE by SWC is the better choice for a reduced complexity LMMSE channel estimator.

4 Conclusions

The LMMSE by SWC estimation algorithm can reduce computational complexity of the traditional LMMSE channel estimator by more than 50% and it outperforms the LMMSE by SVD when channel delay spreads exceeding 50 ns.

References

[1] I. Tolochko and M. Faulkner, "Real Time LMMSE Channel Estimation for Wireless OFDM Systems with Transmitter Diversity", in *Proc. 56th IEEE VTC*, Vancouver, Canada, pp. 1555 – 1559, 2002.

[2] O. Edfors, M. Sandell, J.-J. van de Beek, S.K. Wilson and P.O. Börjesson, "Analysis of DFT-Based Channel Estimators for OFDM", *Wireless Personal Communications*, 12(1), pp. 55 – 70, 2000.

[3] O. Edfors, M. Sandell, J.J. van de Beek, S.K. Wilson and P.O. Börjesson, "OFDM Channel Estimation by Singular Value Decomposition", *IEEE Trans. Commun.*, 46,(7), pp. 931 – 939, 1998.

[4] R. van Nee and R. Prasad, *OFDM for Wireless Multimedia Communications*, Artech House: USA, 2000.

[5] IEEE Std 802.11a/D7.0, "Part 11: Wireless LAN Medium Access Control (MAC) and Physical Layer (PHY) Specifications: High-Speed Physical Layer in the 5 GHz Band", New York, USA, 1999.

[6] L.L. Scharf, *Statistical Signal Processing: Detection, Estimation, and Time Series Analysis*, Addison-Wesley, Inc.: USA, 1991.

[7] J. Medbo and P. Schramm, "Channel Models for HIPERLAN/2 in Different Indoor Scenarios", ETSI BRAN doc. No. 3ER1085B, 1998.

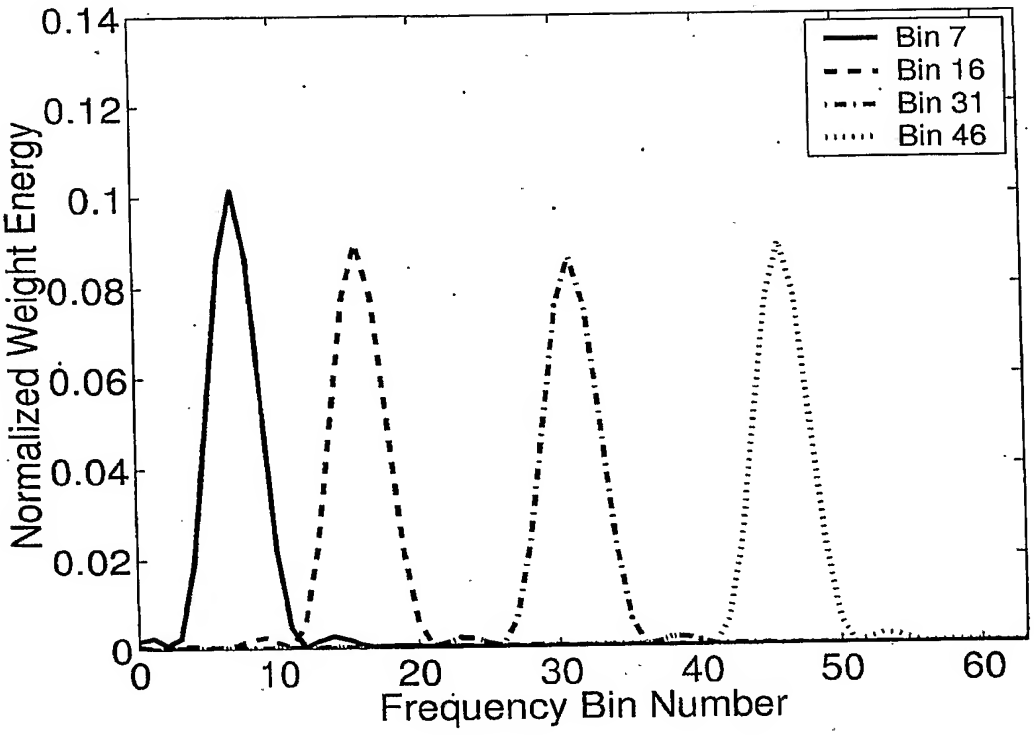

Figure 1: Normalized energy of weights for arbitrary chosen rows from the LMMSE fixed weighting matrix generated for 64-point OFDM.

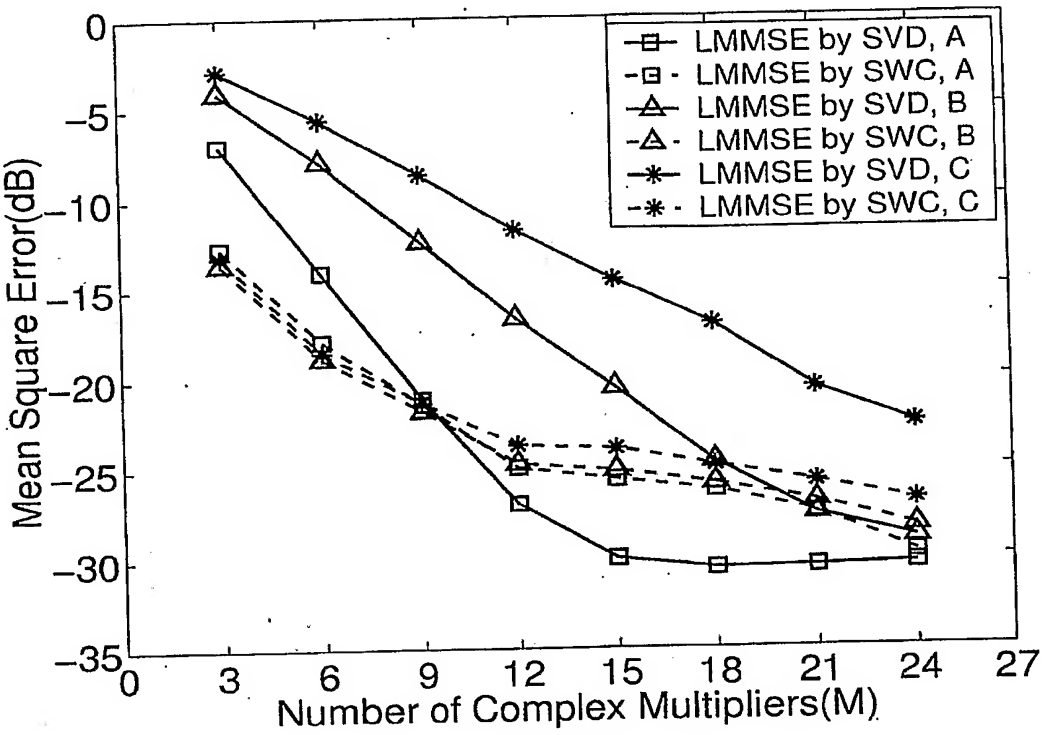

Figure 2: LMMSE by SVD and LMMSE by SWC MSE performance in a 2×1 diversity scheme for a different number of complex multipliers in channels A, B and C at SNR. =.25 dB.

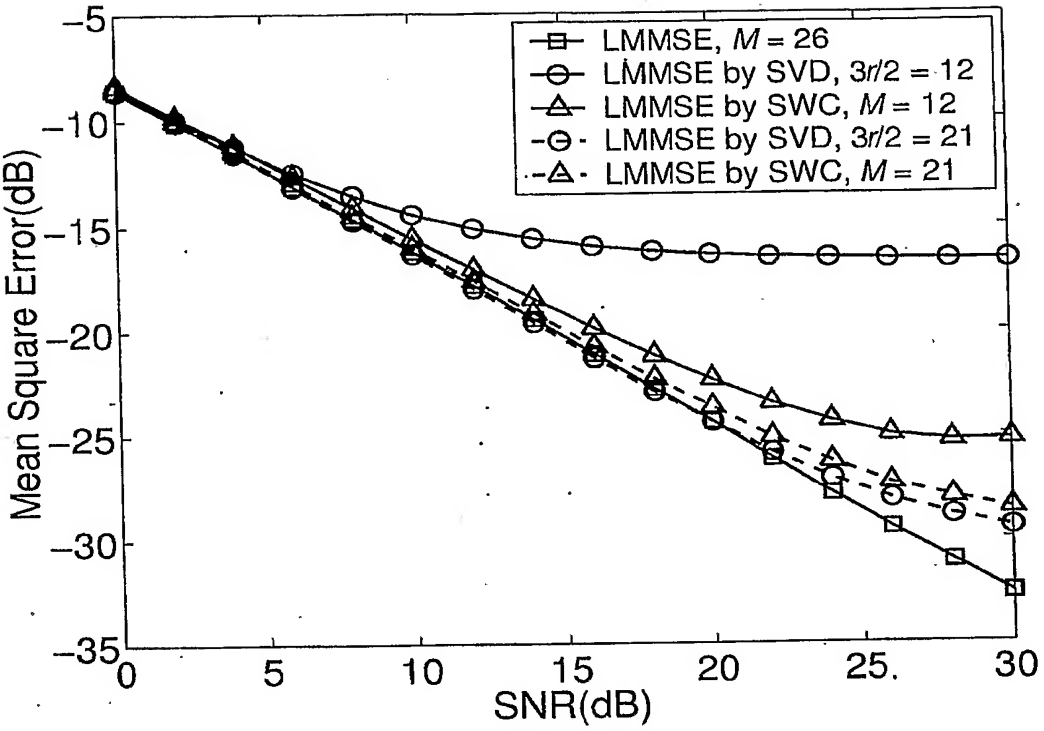

Figure 3: LMMSE and LMMSE with the sparse approximations of the fixed weighting matrix MSE performance in a 2×1 diversity scheme for channel B ($\tau_{rms} = 100$ ns).

Channel Estimation in Wireless LANs with Transmitter Diversity

I. TOLOCHKO and M. FAULKNER.

Australian Telecommunications Cooperative Research Centre, Victoria University, P.O. Box 14428, Melbourne City, VIC, 8001, Australia.
E-mail: igor@sci.vu.edu.au

Abstract: Three pilot symbol architectures are compared in an orthogonal frequency division multiplexing (OFDM) system for a down link diversity environment. The first architecture is called a standard pilot scheme, in which two long pilot symbols (similar to 802.11a) are transmitted on interleaved sub-carriers from Q transmit antennas. The second architecture extends the standard scheme by interleaving the two pilot symbols in the time domain as well as the frequency domain. Each pilot symbol is preceded with a single cyclic prefix (CP) of length 800 ns. The third architecture interleaves a single pilot symbol with a CP of length 1600 ns, over twice the number of sub-carriers than the two preceding architectures. The modified architectures always outperform the standard pilot scheme in HIPERLAN/2 channel environment, since they reduce the interpolation error. No additional pilot overhead (compared to 802.11a) is necessary if the diversity order is low (≤ 2) and the maximum excess delay of a channel is confined to a CP of length 800 ns.

Keywords: channel estimation, orthogonal frequency division multiplexing, singular value decomposition, transmitter diversity, wireless local area networks.

Abbreviations:

BPSK	binary phase shift keying;
CP	cyclic prefix;
FFT	fast Fourier transform;
IDFT	inverse discrete Fourier transform;
ICI	inter-carrier interference;
ISI	inter-symbol interference;
LS	least-squares;
LMMSE	linear minimum mean-square error;
LUT	look-up-table;
MSE	mean square error;
MIMO	multiple-input multiple-output;
NLOS	non-line-of-sight;
OFDM	orthogonal frequency-division multiplexing;
rms	root-mean square;
SISO	single-input single-output;
SNR	signal-to-noise ratio;
SVD	singular value decomposition;
WLANs	wireless local area networks.

1 Introduction

Broadband wireless local area networks (WLANs), such as IEEE 802.11a and HIPERLAN/2, incorporate two long OFDM pilot symbols at the beginning of a data packet, which enable channel estimation [1]. The pilot symbols are preceded with a double length cyclic prefix (CP) to effectively eliminate inter-symbol interference (ISI) and inter-carrier interference (ICI) due to a fading channel. The following work investigates a number of modified pilot schemes, so that transmitter diversity or multiple-input multiple-output (MIMO) systems can be included within existing OFDM standards. Such diversity schemes mitigate fading in channels and improve capacity [2]. However, channel estimation for OFDM systems provides a challenging trade-off between channel estimation accuracy and pilot symbol overhead. To maintain the same pilot symbol overhead as specified by 802.11a, interleaved sub-channels can be used as an orthogonal set of signals to identify each of the transmitting paths [3]. Nonetheless, if the number of transmit antennas is large, the required frequency domain interpolation can degrade the system performance, forcing the use of additional pilot symbols.

2 System Model

Three sub-channel interleaving schemes with Q transmitters and one receiver, requiring an equal average power from each transmit antenna are compared, within the 802.11a OFDM framework. The first scheme consists of a standard pilot system in which two repeated (long) pilot symbols are preceded with a double length CP of 1600 ns, similar to 802.11a. The first modified scheme (modified-1) splits the two repeated pilot symbols into two independent pilot symbols, each preceded with a single CP of length 800 ns. The second modified scheme (modified-2) transmits a single pilot symbol preceded by a CP of 1600 ns, over twice the number of sub-channels, but half the bandwidth of the first two schemes. These three schemes are shown in Figure 1, for a 4×1 antenna diversity system. The first two schemes form two consecutive OFDM pilot

symbols $x_j(i),\ i = (0,\ 1)$ for each antenna $j = (1,\ 2,\ \ldots,\ 4)$. The third scheme forms only one pilot symbol $x_j(i),\ i = 0$ for each antenna j. All three schemes have a preamble length of 8 μs.

The binary phase shift keying (BPSK) modulated pilot tones are split into four interleaved subsets (one subset for each antenna) within the time and frequency grids of the OFDM pilot symbols, so that $\{\mathbf{x}_1(i),\ \mathbf{x}_2(i),\ \mathbf{x}_3(i),\ \mathbf{x}_4(i) \in \mathbf{x}(i)\}$, $\{\mathbf{x}_1(i) \cap \mathbf{x}_2(i) \cap \mathbf{x}_3(i) \cap \mathbf{x}_4(i) = \emptyset\}$ and $\{\mathbf{x}_1(i) \cup \mathbf{x}_2(i) \cup \mathbf{x}_3(i) \cup \mathbf{x}_4(i) = \mathbf{x}(i)\}$. The channel characteristics can be identified in the non-measured sub-channels, by interpolating between the different sets of measured sub-channels from the specified transmit antenna. With these three schemes, the performance of a linear minimum mean-square error (LMMSE) channel estimator and its counterpart, a reduced complexity low rank-r approximation by singular value decomposition (SVD), are analysed by simulations based on HIPERLAN/2 non-sample-spaced channel models [4]. Some of these models (C, D and E) have a channel impulse response with a maximum excess delay, τ_x of the power delay profile, which exceeds a single CP length and in channel E exceeds a double CP length.

When the channel impulse response exceeds a CP length, there are additional sources of interference caused by the ISI term from the preceding symbol and ICI term from the present symbol. Each of these two terms can be modelled as an additional source of uncorrelated additive complex Gaussian noise, with zero mean and combined variance of the channel impulse response taps that exceed the CP length [5], [6].

Under this assumption, the complex base-band channel impulse response of a wireless multipath channel, in which the first L taps are within the CP length and the remaining M taps are outside the CP, can be described by:

$$h(t) = \sum_{l=0}^{L-1} \gamma_l \delta(t - \tau_l) + \sum_{m=L}^{M-1} \gamma_m \delta(t - \tau_m), \tag{1}$$

where τ_l and τ_m are the delays at the lth and mth path respectively, γ_l and γ_m are the corresponding complex gains and $\delta(\tau)$ is the Dirac delta function. With the power of the impulse

response normalised to unity, the variance $\eta_m(k)$ of the interference power due to ISI and ICI in the kth sub-carrier for BPSK, caused by the mth path, can be given by [5]:

$$\eta_m(k) = 2|\gamma_m|^2. \tag{2}$$

The frequency domain input-output description of a received signal $y(k)$ for the kth sub-carrier in a $Q \times 1$ diversity scheme, when Q transmit antennas simultaneously send unique OFDM symbols, each modulated by $x_j(k)$, can be given by:

$$y(k) = \sum_{j=1}^{Q} H_j(k)x_j(k) + w(k) + e(k), \tag{3}$$

where j denotes the transmitter number, $H_j(k)$ is the channel frequency response corresponding to antenna j. $w(k)$ is the additive complex Gaussian noise with zero mean and variance one. $e(k)$ is the interference term presented by the additive complex Gaussian noise with zero mean and variance of $\eta(k)$, given by:

$$\eta(k) = \sum_{m=L}^{M-1} \eta_m(k). \tag{4}$$

HIPERLAN/2 channel paths are non-sample-spaced, resulting in channel impulse response smearing. This is because $H_j(k)$ is the sampled version of the continuous Fourier transform of the channel $h(t)$ and an inverse discrete Fourier transform (IDFT) of $H_j(k)$ is no longer confined to the CP. However the system orthogonality in the continuous time channels is preserved by the only requirement to have a length that is less than the CP [7]. Therefore, the estimation accuracy of the frequency domain LMMSE estimator (and its counterpart the low rank-r approximation by SVD) is not affected by the energy leakage between the channel impulse response taps. On the contrary, the additional term $e(k)$ in equation (3) reduces the quality of the received signal $y(k)$ and therefore the channel estimation accuracy for the ISI/ICI channels. When comparing the three pilot schemes, it is not obvious whether the improvement in interpolation performance

of the modified-1 pilot scheme would outweigh the additional ISI/ICI error term caused by the single (reduced length) CP. Simulations were carried out to compare the three pilot schemes in terms of the mean square error (MSE).

3 Processing Method

In the OFDM-BPSK system with transmitter diversity the LMMSE channel estimation vector $\hat{\mathbf{H}}_j$ corresponding to the jth transmitter can be obtained as follows [8], [9]:

$$\hat{\mathbf{H}}_j = \left[\mathbf{R}_{\mathbf{H}_j\mathbf{P}_j}\left(\mathbf{R}_{\mathbf{P}_j\mathbf{P}_j} + \frac{1}{SNR}\mathbf{I}\right)^{-1}\right]\tilde{\mathbf{P}}_j, \tag{5}$$

where $\mathbf{R}_{\mathbf{H}_j\mathbf{P}_j}$ is the cross-correlation matrix between the channel attenuations $\mathbf{H}_j$ and channel attenuations $\mathbf{P}_j$ at the pilot positions. $\mathbf{R}_{\mathbf{P}_j\mathbf{P}_j}$ is the auto-correlation matrix of the channel attenuations $\mathbf{P}_j$ at the pilot positions. $\mathbf{I}$ is the identity matrix and SNR is the expected value of signal-to-noise ratio (SNR). $\tilde{\mathbf{P}}_j$ is the least-squares (LS) estimation vector at the pilot positions corresponding to antenna j.

In channels with a limited mobility, the $\tilde{\mathbf{P}}_j$ of the two repetitive OFDM symbols in the standard pilot scheme, Figure 1(a), can be obtained as follows:

$$\tilde{\mathbf{P}}_j = \frac{1}{2}\mathbf{X}_j^{-1}\sum_{i=0}^{1}\mathbf{y}_j(i), \tag{6}$$

where $\mathbf{X}_j = \mathbf{X}_j(i), i = (0,1)$ is a diagonal matrix of size $K/Q \times K/Q$ containing the transmitted pilot points $x_j(k)$.

The $\tilde{\mathbf{P}}_j$ in the modified-1 pilot scheme, Figure 1(b), can be obtained by:

$$\tilde{\mathbf{P}}_j = \bar{\mathbf{P}}_j(0) \cup \bar{\mathbf{P}}_j(1), \tag{7}$$

where $\bar{\mathbf{P}}_j(i)$ is the LS estimates vector of length K/Q, corresponding to the ith received pilot OFDM symbol from transmitter j, given by:

$$\bar{\mathbf{P}}_j(i) = \mathbf{X}_j^{-1}(i)\mathbf{y}_j(i). \tag{8}$$

Equation (8) also represents the LS estimation vector $\bar{\mathbf{P}}_j = \bar{\mathbf{P}}_j(i), i = 0$ of length $2K/Q$ for the modified-2 pilot scheme shown in Figure 1(c). With $2K$ sub-carriers, this scheme requires a twofold increase for the correlation matrix size and FFT lengths, when calculating $\hat{\mathbf{H}}_j$ and $\mathbf{y}_j(i)$ respectively.

If the root-mean square (rms) delay spread of the power delay profile τ_{rms} and SNR are set to fixed nominal (expected) values [9], then the fixed weighting matrix (the expression in the square brackets of (5)) needs to be calculated just once and can be stored in a look-up-table (LUT).

The HIPERLAN/2 channels have a τ_{rms} ranging between 50 ns and 250 ns and a mobile terminal speed ranging between 0 m/s and 3 m/s [4]. The time domain correlation remains high for the first two OFDM pilot symbols, using the specified Jake's Doppler spectrum, given by a time domain correlation function $r_t(i)$:

$$r_t(i) = J_0(2\pi T_S f_D i), \tag{9}$$

where $J_0(\cdot)$ is the zeroth order Bessel function of the first kind, T_S is the OFDM symbol duration and f_D is a maximum Doppler frequency, given by:

$$f_D = \frac{v f_c}{C}, \tag{10}$$

where v is the mobile terminal speed; f_c is the carrier frequency and C denotes speed of light. For example, a system with a carrier frequency $f_c = 5\ GHz$ and a terminal speed at 3 m/s,

$f_D = 50\ Hz$. Given a correlation function at $r_t(0) = 1$, we can find from (9) that $r_t(1) = 0.9999996$ when $T_S = 4\ \mu s$. Hence, the $\bar{\mathbf{P}}_j(i)$ remains unchanged in equations (6) and (7) for the two consecutive pilot symbols. However, the frequency domain correlation depends on the multipath channel delay spread [7] and can be described by a frequency domain correlation function $r_f(k)$. For an exponentially decaying multipath power delay profile $r_f(k)$ can be given by [8]:

$$r_f(k) = \frac{1}{1 + j2\pi\tau_{rms}k(\Delta f)}, \tag{11}$$

where Δf denotes the sub-carrier spacing. For example, a system with sub-carrier spacing $\Delta f = 312.5\ kHz$ and τ_{rms} ranging between 0 ns and 250 ns, the correlation $r_f(k)$ is shown in Figure 2 for the first 9 sub-carriers. As the delay spread τ_{rms} of a multipath channel increases, the coherence bandwidth of the channel decreases, resulting in larger interpolation errors for the estimation approach given by (5). This is particularly true for high diversity orders (≥ 4), where the measured sub-carrier separation becomes significant.

With these considerations, a correlation function $r_H(i,k)$ of different pilot symbols i and sub-carriers k for an 802.11a OFDM system in the HIPERLAN/2 channel environment can be simplified to $r_f(k)$ as follows:

$$r_H(i,k) = r_t(i)r_f(k) \cong r_f(k), \tag{12}$$

for $i = 0,\ 1$ and $k = 0,\ 1,\ \ldots,\ K-1$.

4 Low-Rank Approximations

LMMSE processing (5) requires K/Q multiplications per tone in the standard pilot scheme, SK/Q multiplications in the modified-1 pilot scheme (considering diversity orders $Q \geq 2$) and $2K/Q$ in the modified-2 pilot scheme. Where S denotes the number of pilot symbols (and

also the time diversity order) each preceded by the CP. To further reduce the computational complexity, the low-rank approximation can be used. It is found from the correlation matrices that $\mathbf{R}_{\mathbf{H}_j\mathbf{P}_j} = \mathbf{R}_{\mathbf{H}_j\tilde{\mathbf{P}}_j}$ and $\mathbf{R}_{\tilde{\mathbf{P}}_j\tilde{\mathbf{P}}_j} = \left(\mathbf{R}_{\mathbf{P}_j\mathbf{P}_j} + \frac{1}{SNR}\mathbf{I}\right)$ [9].

Equation (5) can be rewritten as follows:

$$\hat{\mathbf{H}}_j = \mathbf{R}_{\mathbf{H}_j\mathbf{P}_j}\mathbf{R}^{-1}_{\tilde{\mathbf{P}}_j\tilde{\mathbf{P}}_j}\mathbf{R}^{1/2}_{\tilde{\mathbf{P}}_j\tilde{\mathbf{P}}_j}\mathbf{R}^{-1/2}_{\tilde{\mathbf{P}}_j\tilde{\mathbf{P}}_j}\tilde{\mathbf{P}}_j. \tag{13}$$

The best low-rank approximation of $\mathbf{R}_{\mathbf{H}_j\mathbf{P}_j}\mathbf{R}^{-1}_{\tilde{\mathbf{P}}_j\tilde{\mathbf{P}}_j}\mathbf{R}^{1/2}_{\tilde{\mathbf{P}}_j\tilde{\mathbf{P}}_j}$ is given by the SVD [10]:

$$\mathbf{R}_{\mathbf{H}_j\mathbf{P}_j}\mathbf{R}^{-1}_{\tilde{\mathbf{P}}_j\tilde{\mathbf{P}}_j}\mathbf{R}^{1/2}_{\tilde{\mathbf{P}}_j\tilde{\mathbf{P}}_j} = \mathbf{U}_j\mathbf{\Sigma}_j\mathbf{V}_j^H, \tag{14}$$

where $\mathbf{U}_j$ and $\mathbf{V}_j^H$ are unitary matrices, and $\mathbf{\Sigma}_j$ is a diagonal matrix with the singular values corresponding to antenna j. The superscript $(\cdot)^H$ denotes Hermitian transpose.

The rank-r estimator is then defined by:

$$\hat{\mathbf{H}}_j = \mathbf{U}_j \begin{bmatrix} \mathbf{\Sigma}_j^r & 0 \\ . & \\ 0 & 0 \end{bmatrix} \mathbf{V}_j^H\mathbf{R}^{-1/2}_{\tilde{\mathbf{P}}_j\tilde{\mathbf{P}}_j}\tilde{\mathbf{P}}_j, \tag{15}$$

where $\mathbf{\Sigma}_j^r$ is the $r \times r$ upper left corner of $\mathbf{\Sigma}_j$, containing the strongest singular values. The superscript $(\cdot)^r$ denotes rank-r.

Similarly with the weighting matrix in Equation (5), the fixed weighting matrix in (15) needs to be calculated only once and can be stored in a LUT. However, the low rank-r approximation causes an irreducible error floor [9]. To eliminate this error floor within a given SNR range, the rank-r needs to be sufficiently large, i.e. a trade off between the estimator complexity and estimator accuracy, particularly at high SNRs. An appropriate value for r is obtained when it is within the CP range [9]. On the other hand, singular value spread depends on the channel power delay profile. Larger rms delay spreads in the channel, result in less singular value spreads, which require a higher rank-r. Whilst smaller rms delay spreads in the channel produce

larger singular value spreads, requiring a lower rank-r.

This is illustrated in Figure 3 for various rms delay spreads of the HIPERLAN/2 channel models obtained from $\mathbf{R}_{\mathbf{H}_j\mathbf{H}_j}$. By implementing the switched LUT approach described in previous work [3], the appropriate rank-r can be chosen based on coarse estimates of τ_{rms} and SNR.

5 Complexity Analysis

The complexity involved in channel estimation computation, (5) and (15), is presented in terms of the effective matrix size and number of complex multiplications required for one antenna j. This is summarized in Table I for the three pilot symbol schemes with transmitter diversity order Q, ranging from 2 to 8. The pilot symbol overhead is identical to an 802.11a system.

To illustrate complexity contributed by the LS estimation, the required complex multiplications are also included in Table I. The standard pilot scheme requires K/Q additional multiplications, the modified-1 pilot scheme, SK/Q multiplications and the modified-2 pilot scheme, $2K/Q$ multiplications for one antenna j.

Analysis of the entries in Table I, shows that the standard pilot scheme is less complex than the modified pilot schemes for a given diversity order Q for both the LMMSE and optimal low rank-r approximation. This is due to a different LS estimation approach taken in the modified-1 pilot scheme (7) and an increased sub-carrier number in the modified-2 pilot scheme. Both modified pilot schemes reduce the interpolation error (refer to Figure 2), at the expense of processing complexity. The modified schemes require $(K/Q + 1/2)$ more complex multiplications for LMMSE processing. While the low rank-r approximation of the modified schemes require $(r/Q + 1/2)$ and $(3r/Q + 1/2)$ more complex multiplications, for the modified-1 and modified-2 schemes respectively.

When the channel impulse response of a fading channel is confined to the single CP length, all three pilot schemes remain ISI/ICI error free. For a 2×1 diversity system, the modified-1

pilot scheme remains also an interpolation error free. Given that $S = Q$, all K LS attenuations are available for both LMMSE (5) and low rank-r estimator (15) processing. When the channel impulse response exceeds the single CP length, the longer CP and closer spacing between the sub-carriers of the modified-2 pilot scheme can improve the estimator performance by eliminating the ISI/ICI error term $e(k)$ and by reducing the interpolation error.

6 Simulation Results

The MSE_j of an LMMSE estimator (5) and optimal low rank-r estimator (15) are analysed by simulation. The MSE_j corresponding to the $\hat{\mathbf{H}}_j$ is given by [7]:

$$MSE_j = \frac{1}{K} trace(\Psi_j), \tag{16}$$

where Ψ_j is the auto-covariance matrix of the estimation error for antenna j, given by:

$$\Psi_j = E\left\{\left(\hat{\mathbf{H}}_j - \mathbf{H}_j\right)\left(\hat{\mathbf{H}}_j - \mathbf{H}_j\right)^H\right\}. \tag{17}$$

The MSE channel estimation performance was evaluated by sending 2000 OFDM-BPSK pilot symbols in an 802.11a system. The standard/modified-1 schemes used 52 sub-channels (out of a possible $K = 64$), while the modified-2 scheme used 104 sub-channels (out of a possible $2K = 128$). A sampling rate of $f_s = 20\ MHz$, and a CP length of 16 (800 ns) and 32 (1600 ns) samples were used in the modified-1 and standard/modified-2 pilot schemes respectively. HIPERLAN/2 non-line-of-sight (NLOS) channels (A, B, C and E) were used and a transmitter diversity of order of 2, 4 and 8 analysed. It was assumed that perfect knowledge of the SNR and rms delay spread τ_{rms} were available for the calculation of the weighting matrices from (5) and (15) [7].

The MSE performance of the three channel estimation schemes is presented in Figure 4 and

Figure 5 for the LMMSE (5) estimator in a 4×1 diversity scheme. The modified pilot schemes outperform the standard pilot scheme for all cases, at the expense of increased computational complexity. In the modified pilot schemes ($K/4+1/4$) more complex multiplications per tone are required. Also, the modified-2 pilot scheme adds more complexity for $\mathbf{y}_j(i)$ calculation requiring twofold increase of FFT size. The MSE error floor rises with the delay spread, as the channel's coherence bandwidth decreases. The standard scheme exhibits the most significant error floor, because of the greater spacing between the pilot tones, resulting in larger interpolation errors. ISI/ICI also introduces an error floor in the modified-1 pilot scheme at high SNRs for channel C in Figure 5 as a result of the reduced CP length. The modified-2 pilot scheme has the lowest error floor because of the longer CP length and lower interpolation error.

The channel estimation systems need to operate effectively while maintaining an MSE that does not dominate the receiver noise performance. For performance analysis a simple single-input single-output (SISO) LS channel estimation, obtained from two long OFDM pilot symbols, is used as the bound for acceptable performance (MSE $= -$(SNR$+3$) dB). The SNR boundary where the MSE is acceptable (requiring no additional pilot overhead) for the LMMSE estimator (5) is given in Table II, for 2×1, 4×1 and 8×1 diversity schemes, based on HIPERLAN/2 channels. The ISI/ICI free channels A and B (considering the single CP length) require no additional pilots for all practical SNR values, when the diversity order is low (≤ 2), however, when the diversity order is increased (SNR ≤ 5 dB, for 8×1 system and channel B) the usable SNR range is reduced. The effect of longer delay spreads (channels C and E) further reduces the usable SNR dynamic range, making all diversity orders impractical using 802.11a pilot symbol overhead in both standard and modified pilot schemes. It should be noted that the modified-2 scheme does not necessarily improve the LS, SISO bound (MSE $= -$(SNR $+ 3$) dB), even though it inherently has a lower error floor for the channels exceeding a single CP. Additional pilot overhead (compared to 802.11a) or an alternative processing approach to the analysed schemes is required for diversity orders of four or above.

To illustrate the performance improvement attainable, Table III presents the SNR boundary for the LMMSE estimator (5) when pilot symbol length is increased to 16 μs (twice the length of 802.11a). With the increased pilot symbol length, a 4×1 diversity system becomes feasible for both A and B channels, and a 2×1 system achievable for all HIPERLAN/2 channel models (except for channel E) using the modified pilot schemes.

In Figure 6, the MSE performance of a 2×1 low rank-r estimator (15) is presented for the modified-1 pilot scheme in HIPERLAN/2 channels A and B. LMMSE performance is also given for a reference. The low rank-r approximation produces an irreducible error floor. To eliminate this error floor for SNRs ≤ 30 dB (a reasonable dynamic range for practical intents), the rank-r is set to a value of $r = 9$ for channel A and $r = 14$ for channel B. The choice of r is based on the rms delay spread of a channel (refer to Figure 3). Although this scheme requires $(r/2+1/2)$ more complex multiplications per tone compared to the standard pilot scheme (refer to Table I), with $r << K/Q$ the added complexity is reduced (weighed against the LMMSE processing). On the other hand, the modified-2 pilot scheme requires $(3r/2 + 1/2)$ additional complex multiplications per tone and twofold increase of FFT size for the received vector $\mathbf{y}_j(i)$ computation, with respect to the standard pilot scheme. Therefore, in channels confined to the CP length, the low rank-r modified-1 pilot scheme is the best compromise in performance versus complexity, especially when the number of the pilot symbols equal to the number of antennas. For example, a 4×1 diversity system would require 4 pilot symbols ($S = Q = 4$), this is twice the pilot symbol overhead of an 802.11a system. Adopting the switched LUT approach described in [3], the appropriate rank-r can be selected, based on coarse estimates of τ_{rms} and SNR.

7 Conclusions

In this paper we have compared three pilot symbol allocation schemes for an 802.11a OFDM system in a down link diversity environment. The standard scheme uses two long pilot symbols

preceded with a CP length of 1600 ns and interleaves the tones in the frequency domain to identify each transmit antenna. The modified-1 pilot scheme extends the standard scheme by interleaving the two pilot symbols in the time domain as well as the frequency domain. Each pilot symbol is preceded with a single CP of length 800 ns. The modified-2 pilot scheme interleaves a single pilot symbol with a CP of length 1600 ns, over twice the number of sub-carriers than the two preceding schemes. The modified pilot schemes always outperform the standard pilot scheme in a HIPERLAN/2 channel environment, since they reduce the interpolation error. No additional pilot overhead (compare to 802.11a) is necessary if the diversity order is low (≤ 2) and the maximum excess delay of the channel is confined to a CP of length 800 ns. The low rank-r modified-1 pilot scheme is the best compromise in performance versus complexity for the ISI/ICI free channels, especially when the number of the pilot symbols equal to the number of antennas.

References

[1] IEEE Std 802.11a/D7.0, "Part 11: Wireless LAN Medium Access Control (MAC) and Physical Layer (PHY) Specifications: High-Speed Physical Layer in the 5 GHz Band", New York, USA, 1999.

[2] Y.G. Li, N. Seshadri and S. Ariyavisitakul, "Channel Estimation for OFDM Systems with Transmitter Diversity in Mobile Wireless Channels", IEEE J. Select Areas Commun., 17(3), pp. 461 – 471, 1999.

[3] I. Tolochko and M. Faulkner, "Real Time LMMSE Channel Estimation for Wireless OFDM Systems with Transmitter Diversity", in Proc. 56th IEEE VTC, Vancouver, Canada, pp. 1555 – 1559, 2002.

[4] J. Medbo and P. Schramm, "Channel Models for HIPERLAN/2 in Different Indoor Scenarios", ETSI BRAN doc. No. 3ER1085B, 1998.

[5] J.L. Seoane, S.K. Wilson and S. Gelfand, "Analysis of Intertone and Interblock Interference in OFDM when the Length of the Cyclic Prefix is Shorter than the Length of the Impulse Response of the Channel", in Proc. IEEE GLOBECOM, Vol. 1, pp. 32 – 36, 1997.

[6] M. Faulkner, "The Effect of Filtering on the Performance of OFDM Systems", IEEE Trans. Veh. Technol., 49(5), pp. 1877 – 1884, 2000.

[7] O. Edfors, M. Sandell, J.-J. van de Beek, S.K. Wilson and P.O. Börjesson, "Analysis of DFT-Based Channel Estimators for OFDM", Wireless Personal Communications, 12(1), pp. 55 – 70, 2000.

[8] R. van Nee and R. Prasad, OFDM for Wireless Multimedia Communications, Artech House: USA, 2000.

[9] O. Edfors, M. Sandell, J.J. van de Beek, S.K. Wilson and P.O. Börjesson, "OFDM Channel Estimation by Singular Value Decomposition", IEEE Trans. Commun., 46,(7), pp. 931 – 939, 1998.

[10] L.L. Scharf, Statistical Signal Processing: Detection, Estimation, and Time Series Analysis, Addison-Wesley, Inc.: USA, 1991.

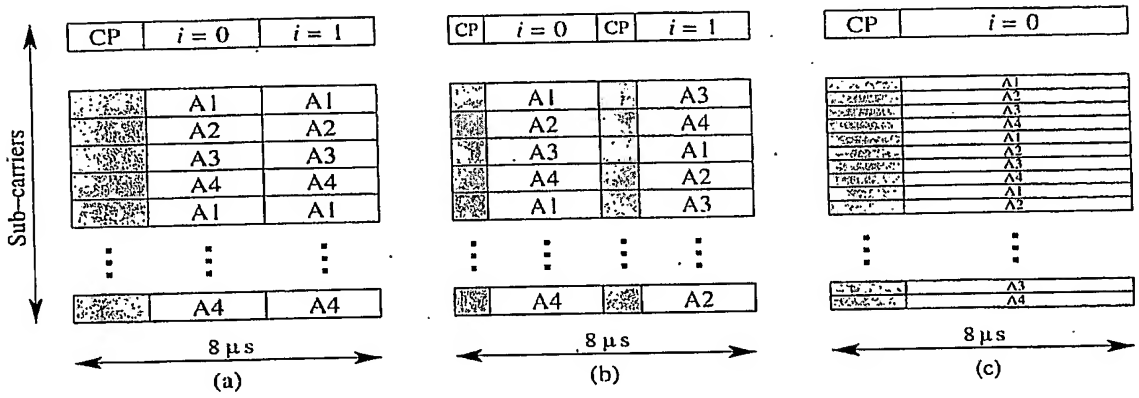

Figure 1: The pilot schemes of the OFDM symbols with distributed sub-carriers between four antennas A1 to A4: (a) the standard pilot scheme with the double length CP, (b) the modified-1 pilot scheme with the single length CP and (c) the modified-2 pilot scheme with $2K$ sub-carriers.

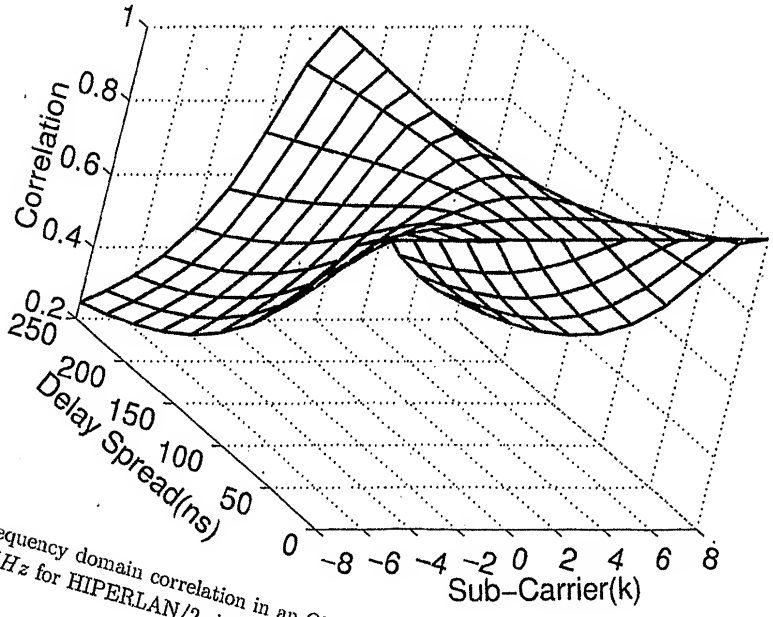

Figure 2: Frequency domain correlation in an OFDM system with $K = 64$ and sampling rate of $fs = 20\ MHz$ for HIPERLAN/2 channels.

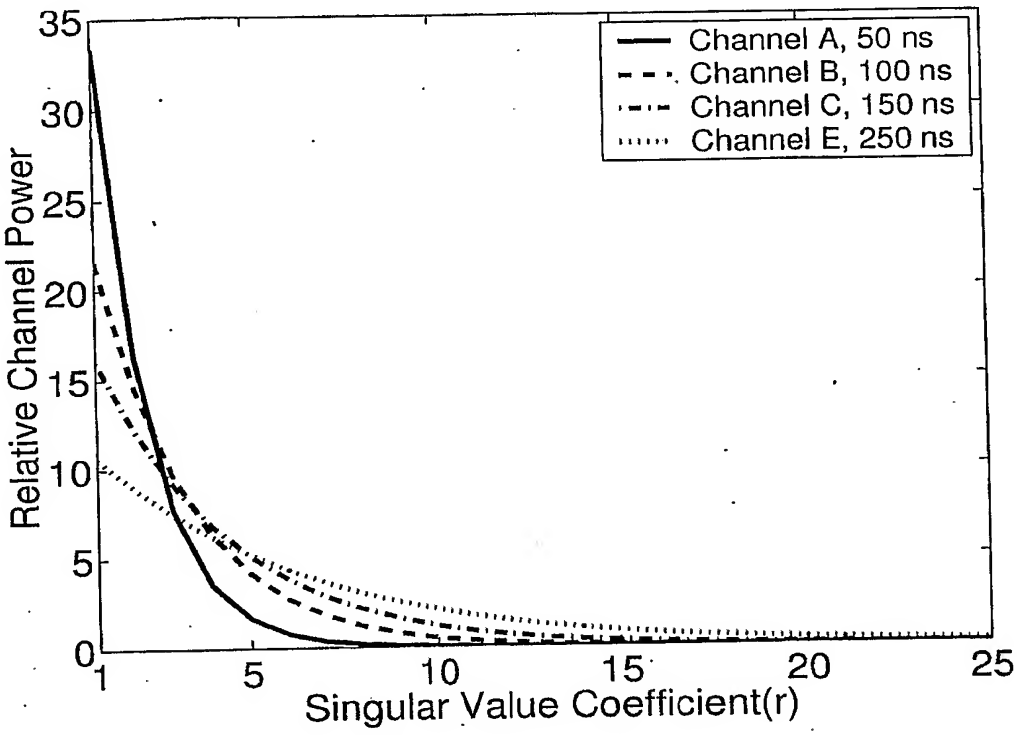

Figure 3: Relative channel power $\Sigma_j(k)/E\{|H_j(k)|^2\}$ of the singular value coefficients in an OFDM system with $K = 64$ and sampling rate of $fs = 20\ MHz$ for various τ_{rms} values ranging from 50 ns to 250 ns.

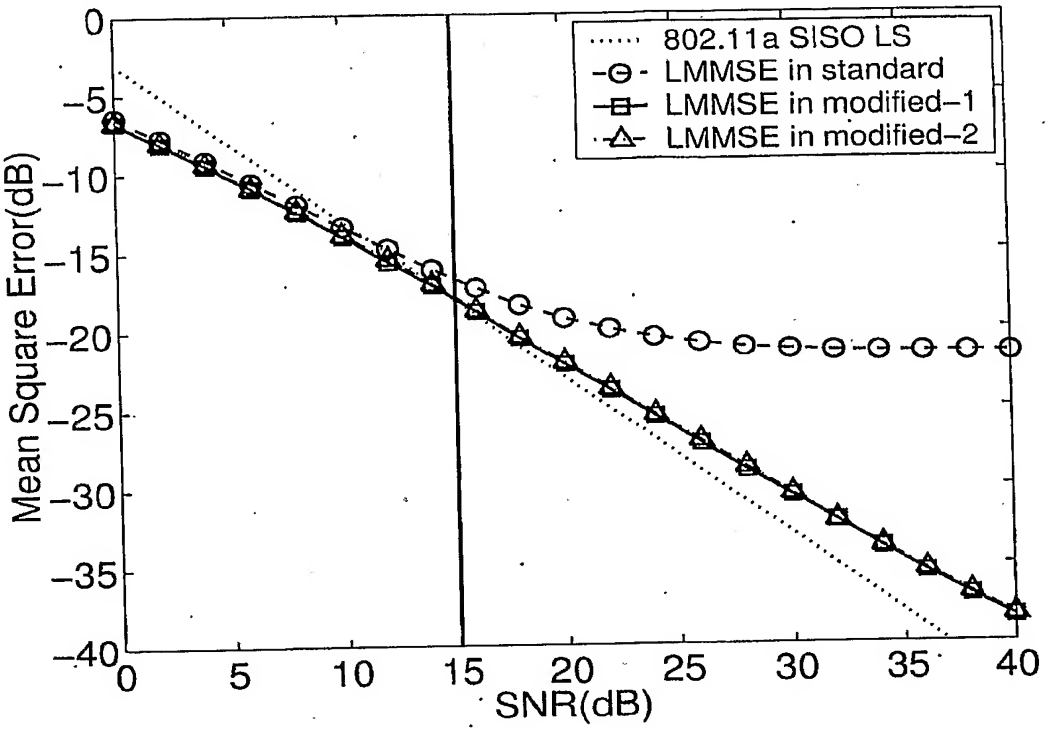

Figure 4: LMMSE channel estimation MSE in a 4×1 diversity scheme for HIPERLAN/2 channel B ($\tau_{rms} = 100\ ns, \tau_x = 730\ ns$).

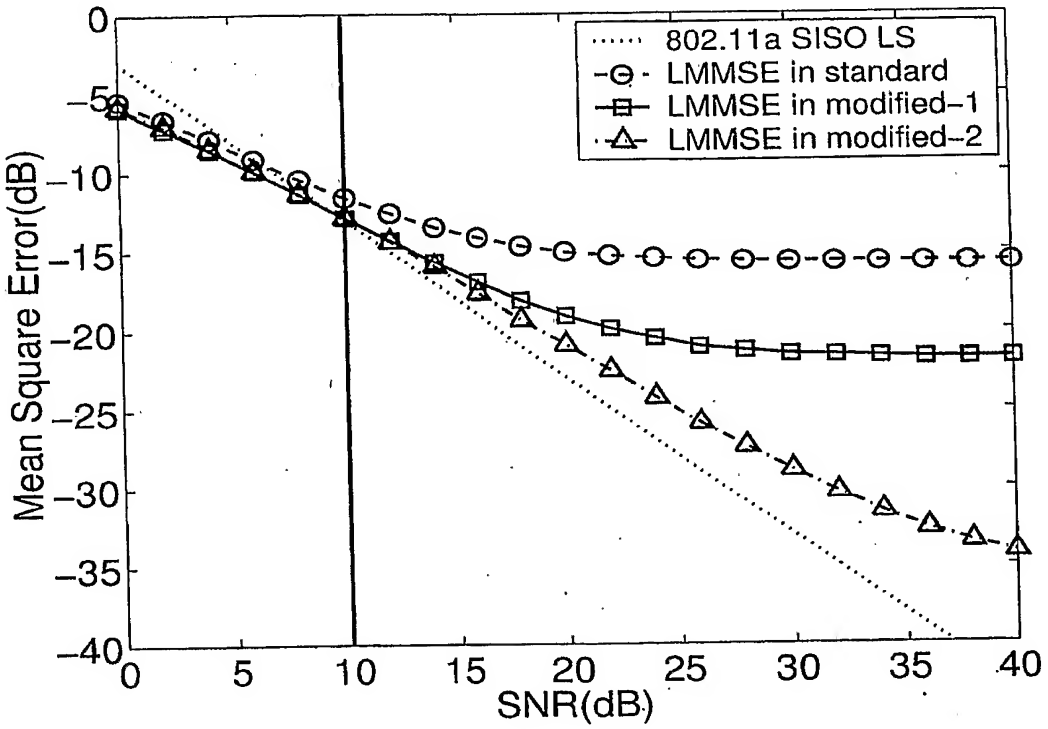

Figure 5: LMMSE channel estimation MSE in a 4×1 diversity scheme for HIPERLAN/2 channel C ($\tau_{rms} = 150\ ns, \tau_x = 1050\ ns$).

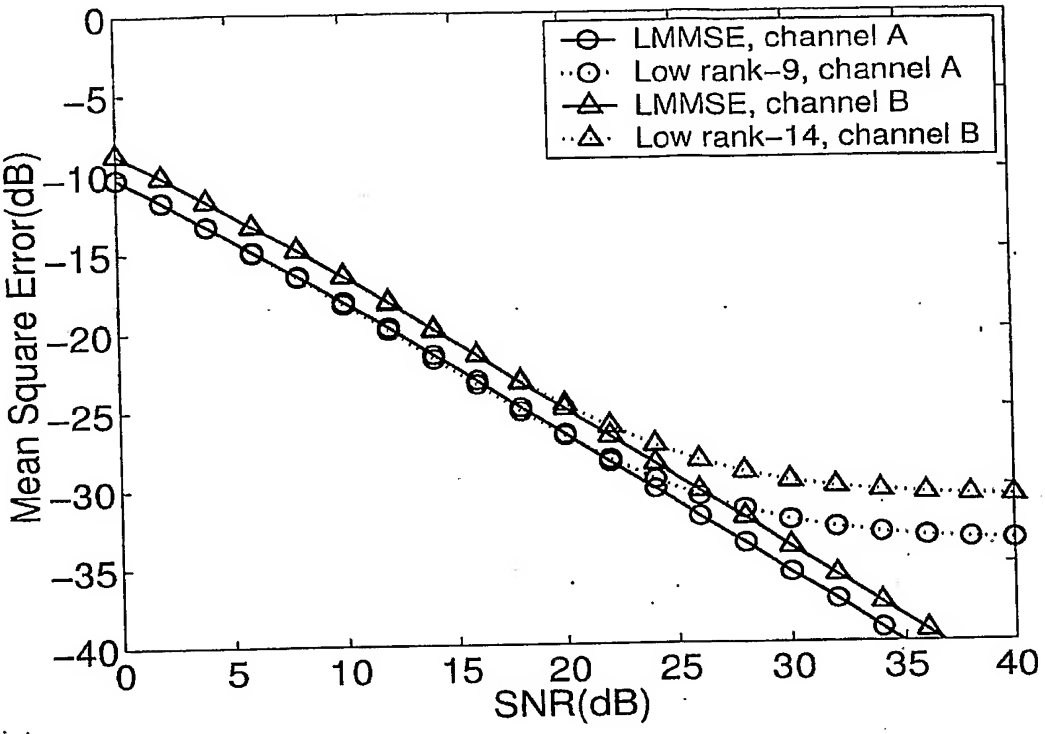

Figure 6: Low rank-r and LMMSE channel estimation MSE of the modified-1 scheme in a 2×1 diversity system for channels A ($\tau_{rms} = 50\ ns, \tau_x = 390\ ns$) and B ($\tau_{rms} = 100\ ns, \tau_x = 730\ ns$).

Table I. Channel Estimator Complexity with 802.11a Pilot Symbol Overhead for jth Antenna

Estimator	2×1		4×1		8×1	
	Matrix size	Multipl. per tone	Matrix size	Multipl. per tone	Matrix size	Multipl. per tone
LMMSE (5) in standard scheme	$K/2 \times K/2$	$K/2+1/2$	$K/4 \times K/4$	$K/4+1/4$	$K/8 \times K/8$	$K/8+1/8$
LMMSE (5) in modified schemes	$K \times K$	$K+1$	$K/2 \times K/2$	$K/2+1/2$	$K/4 \times K/4$	$K/4+1/4$
Low rank-r (15) in standard scheme	$r \times r$	$3r/2+1/2$	$r \times r$	$5r/4+1/4$	$r \times r$	$9r/8+1/8$
Low rank-r (15) in modified-1 scheme	$r \times r$	$2r+1$	$r \times r$	$3r/2+1/2$	$r \times r$	$5r/4+1/4$
Low rank-r (15) in modified-2 scheme	$r \times r$	$3r+1$	$r \times r$	$5r/2+1/2$	$r \times r$	$9r/4+1/4$

Table II. Maximum SNR Range for the LMMSE with 802.11a Pilot Symbol Overhead

HIPERLAN/2 Channel	τ_{rms} (ns)	SNR (dB)		
		2×1	4×1	8×1
A	50	> 37 (A)	27 (M1)	10.5 (M1)
B	100	> 37 (M1, M2)	15 (M1, M2)	5 (M1, M2)
C	150	25 (M2)	10 (M1, M2)	2.5 (M1, M2)
E	250	13.5 (M2)	4.5 (M1, M2)	1 (M1, M2)

A – any pilot symbol scheme; M1 – modified-1 pilot symbol scheme; M2 – modified-2 pilot symbol scheme.

Table III. Maximum SNR Range for the LMMSE with Pilot Symbol Overhead of 16 μs

HIPERLAN/2 Channel	τ_{rms} (ns)	SNR (dB)		
		2×1	4×1	8×1
A	50	> 37 (A)	> 37 (M1, M2)	27 (M1)
B	100	> 37 (M1, M2)	> 37 (M1, M2)	15 (M1, M2)
C	150	> 37 (M1, M2)	25 (M2)	10 (M1, M2)
E	250	24.5 (M1, M2)	13.5 (M2)	4.5 (M1, M2)

A – any pilot symbol scheme; M1 – modified-1 pilot symbol scheme; M2 – modified-2 pilot symbol scheme.